

Identification of a Novel Mutation in the *CDHR1* Gene in a Family With Recessive Retinal Degeneration

Jacque L. Duncan, MD; Austin Roorda, PhD; Mili Navani; Sangeetha Vishweswaraiah, MSc; Reema Syed, MBBS; Shiri Soudry, MD; Kavitha Ratnam, BS; Harini V. Gudiseva, MSc, MS; Pauline Lee, PhD; Terry Gaasterland, PhD; Radha Ayyagari, PhD

Objectives: To describe the clinical phenotype and identify the molecular basis of disease in a consanguineous family of Palestinian origin with autosomal recessive retinal degeneration.

Methods: Eight family members were evaluated with visual acuity and perimetry tests, color fundus photographs, full-field electroretinography, and optical coherence tomography. Cone photoreceptors surrounding the fovea were imaged in 2 members, using adaptive optics scanning laser ophthalmoscopy. Exome was captured using probes and sequenced. Readings were mapped to reference hg19. Variant calls and annotations were performed, using published protocols. Confirmation of variants and segregation analysis was performed using dideoxy sequencing.

Results: Analysis detected 24 037 single-nucleotide variants in one affected family member, of which 3622 were rare and potentially damaging to encoded proteins. Further analysis revealed a novel homozygous nonsense change, c.1381 C>T, p.Gln461X in exon 13 of the *CDHR1*

gene, which segregated with retinal degeneration in this family. Affected members had night blindness beginning during adolescence with progressive visual acuity and field loss and unmeasurable electroretinographic responses, as well as macular outer retinal loss, although residual cones with increased cone spacing were observed in the youngest individual.

Conclusions: Exome analysis revealed a novel *CDHR1* nonsense mutation segregating with progressive retinal degeneration causing severe central vision loss by the fourth decade of life. High-resolution retinal imaging revealed outer retinal changes suggesting that *CDHR1* is important for normal photoreceptor structure and survival.

Clinical Relevance: Exome sequencing is a powerful technique that may identify causative genetic variants in families with autosomal recessive retinal degeneration.

Arch Ophthalmol. 2012;130(10):1301-1308

Author Affiliations:

Department of Ophthalmology, UCSF (University of California, San Francisco), San Francisco (Drs Duncan, Syed, and Soudry and Ms Ratnam), Vision Science Graduate Group, School of Optometry, UC Berkeley, Berkeley (Dr Roorda), Shiley Eye Center (Mss Navani, Vishweswaraiah, and Gudiseva and Dr Ayyagari) and Institute for Genomic Medicine, UC San Diego, San Diego (Dr Gaasterland), and Department of Molecular and Experimental Medicine, The Scripps Research Institute (Dr Lee), La Jolla, California.

RECESIVE RETINAL DEGENERATIONS (RDs) are a genetically heterogeneous group of hereditary conditions. At least 56 genes associated with these conditions have been identified.¹ Mutations in some of these genes are associated with multiple phenotypes.²⁻⁵ The large number of genes implicated in causing these degenerations, in addition to allelic and phenotypic heterogeneity, complicate the molecular and clinical diagnoses of RDs and demonstrate the need for screening all genes associated with these phenotypes.

Most variants implicated in causing diseases are located in the coding regions of the genome, the exome,⁶ and sequencing the entire exome has been a useful tool for the identification of mutations causing mendelian inherited diseases.⁷ Exome se-

quencing also allows efficient screening of all genes known to be associated with RD.⁸

Mutations in genes encoding proteins critical for normal photoreceptor structure and function have been implicated in RD. Cadherin-related family member 1 (*CDHR1*; OMIM *609502), previously known as protocadherin 21 (*PCDH21*), is a member of the cadherin family that localizes to the base of the photoreceptor outer segment (OS) at the junction between the inner segments (ISs) and OSs.^{9,10} Targeted disruption of *CDHR1* causes OS disorganization and progressive photoreceptor cell death. Mice homozygous for null mutations in the *CDHR1* gene show normal retinal development and structure at age 1 month but develop photoreceptor cell death beginning at 1 month and progressive photoreceptor loss.¹⁰ Absence of *CDHR1* affects the structure of the

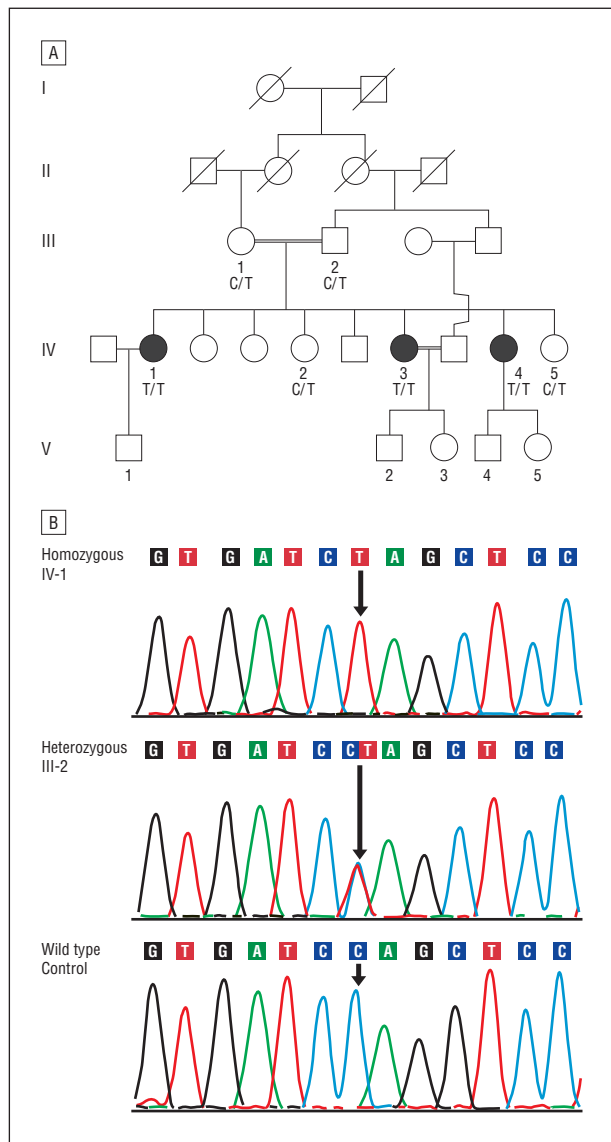


Figure 1. Pedigree and electropherogram of the family studied. A, Pedigree with autosomal recessive retinal degeneration segregates with the c.1381 C>T *CDHR1* mutation. Squares indicate males; circles, females; shaded symbols, retinal degeneration; double lines, consanguinity; and slash marks, individuals who had died. B, Electropherograms with the sequence of the *CDHR1* gene encompassing the c.1381 C/T region showing the homozygous c.1381 C>T change identified in the affected siblings, the sequence of an unaffected family member with the c.1381 C>T change in the heterozygous state, and the wild-type sequence at the c.1381 nucleotide of the *CDHR1* gene.

rod and cone OS, leaving phototransduction largely intact, and the hallmark is disorganized discs and photoreceptor degeneration.¹⁰ Recently, mutations in the *CDHR1* gene mapped to 10q23.1 have been reported^{11,12} in families with autosomal recessive RD affecting both rods and cones and characterized by macular degeneration in the third decade of life (*CORD15* [OMIM #613660]). Histologic studies¹⁰ of retinal structure in mice with *CDHR1* mutations demonstrate abnormalities of OS structure with subsequent photoreceptor degeneration. There have been no histologic studies of human eyes with RD associated with *CDHR1* mutations.

The present study describes exome analysis of an affected member of a consanguineous pedigree with 3 sib-

lings affected with recessive RD and identification of a novel, potentially pathogenic sequence variant in the *CDHR1* gene segregating with the disease. These patients underwent detailed clinical evaluation using high-resolution retinal imaging techniques, including spectral-domain optical coherence tomography (SD-OCT) and adaptive optics scanning laser ophthalmoscopy (AOSLO). These studies yielded insight into how *CDHR1* mutations affect retinal structure in humans and the potential role of *CDHR1* in preserving OS structure and photoreceptor survival.

METHODS

Research procedures were performed in accordance with the Declaration of Helsinki. The study protocol was approved by the UC San Francisco and UC San Diego institutional review boards. A 3-generation consanguineous family of Palestinian Muslim descent with 3 affected female and 5 unaffected (4 female, 1 male) siblings (**Figure 1A**) was studied. Both parents (III-1 and III-2), all 3 affected sisters (IV-1, IV-3, and IV-4), and 2 of the 5 unaffected siblings (IV-2 and IV-5) participated in clinical studies and provided blood samples for genetic analysis; V-1, the son of affected family member IV-1, was available only for clinical examination and did not participate in genetic studies. Other family members were not examined by the authors, but records from eye examinations performed elsewhere were reviewed and data are included in this article.

GENETIC ANALYSIS

Blood samples collected from the parents, all affected siblings, and 3 of the 5 unaffected siblings were examined for isolation of DNA. Exome of patient IV-1 was captured using probes (Nimblegen SeqCap EZ V2.0) and was sequenced (Illumina HiSeq). Readings were mapped to reference hg19, using Bowtie (<http://bowtie-bio.sourceforge.net>). Sequence variants were called using SAMtools (<http://samtools.sourceforge.net/>) and annotated with SeattleSeq Annotation (<http://snp.gs.washington.edu/SeattleSeqAnnotation/>).⁶ All changes present in genes implicated in RD were identified. Previously reported mutations and novel potentially pathogenic changes detected in genes associated with RD were further evaluated by dideoxy sequencing and segregation analysis.

CLINICAL EXAMINATION

A complete history was obtained, including information about all known family members. Measurement of best-corrected visual acuity was performed using a standard eye chart according to the Early Treatment of Diabetic Retinopathy Study protocol. Color vision was examined using the Farnsworth D-15 dichotomous test for color blindness (Psychological Corporation) followed by the Lanthony desaturated D-15 test (Richmond Products, Inc) if there were no crossing errors on the Farnsworth panel; the data were analyzed using a web-based platform scoring method (<http://www.torok.info/colorvision>), and the error scores were calculated using methods proposed by Bowman¹³ and Lanthony¹⁴ for the Farnsworth and Lanthony tests, respectively. The color confusion index was defined as the total color difference score of the participant divided by the normal total color difference score. For the desaturated Lanthony D-15 color test, the total error score was consistent with normal vision if it fell below the 95% confidence level (109 for age 64 years and 51 for age 21 years). Goldmann kinetic perimetry testing was performed with V-4-e and I-4-e targets; when the I-4-e target was

not perceived, the II-4-e and III-4-e targets were used. Axial length was measured noninvasively using partial coherent interferometry with short-coherence infrared (780- μm wavelength) light (Carl Zeiss Meditec AG).

Pupils were dilated with tropicamide, 1%, and phenylephrine, 2.5%, before obtaining color fundus photographs, using a digital camera (Topcon 50EX; Topcon Medical Systems), and SD-OCT images were obtained, using a laser scanning camera (Spectralis HRA+OCT; Heidelberg Engineering), as described previously.¹⁵ Full-field electroretinography was performed after 45 minutes of dark adaptation, using contact lens electrodes (Burian-Allen; Hansen Ophthalmic Development Laboratory), according to International Society for Clinical Electrophysiology of Vision standards¹⁶ and as described elsewhere.¹⁷

AOSLO IMAGE ACQUISITION AND CONE SPACING ANALYSIS

High-resolution images were obtained using AOSLO in each eye, and images were analyzed using custom-written software to determine cone spacing measures, using previously described methods.^{17,18} Cone spacing measures were compared with measures from 24 age-similar healthy individuals, and z scores, or standard deviations from the normal mean, were reported; z scores greater than 2 were considered abnormal.

RESULTS

GENETIC ANALYSIS

Evaluation of the exome sequence of IV-1 detected 24 037 single-nucleotide variants, of which 3622 were rare and potentially damaging to encoded proteins. Further examination of sequence variants observed in genes associated with RD identified a heterozygous variant, c.3899 G>A (p. R1300Q; rs61750129), in the *ABCA4* gene (NG_009073.1 [NCBI Entrez Gene 24]), which has been identified in 2 patients with RD. One of these patients was a compound heterozygote with a P309R mutation; the second patient had no additional *ABCA4* sequence variants.² The frequency of the A allele at c.3899 of *ABCA4* is reported to be 0.022.¹⁹ Analysis of all 3 affected siblings revealed the presence of the c.3899 G>A *ABCA4* variant in 2 affected sisters in the heterozygous state; this variant was absent in the third affected sister. Sequence analysis of the entire coding region of the *ABCA4* gene by dideoxy sequencing revealed no additional potentially pathogenic changes or known causative mutations in IV-1.

Examination of sequence variants also identified a novel homozygous, probably pathogenic c.1381 C>T variant in the *CDHR1* gene (NG_028034.1 [NCBI Entrez Gene 92211]). Segregation analysis of the novel homozygous c.1381 C>T change in the *CDHR1* gene established segregation of this change with RD in this pedigree (Figure 1). This change was detected in the heterozygous state in the parents and unaffected siblings of the affected sisters. This variant was not reported in the 1000 genomes data or in any other single-nucleotide polymorphism database. We also did not find this change in the chromosomes of 100 white individuals. Together, these observations suggest that this is not a common variant in whites and other populations included in the large-scale single-nucleotide variants discovery projects. Analy-

sis of healthy control individuals of Palestinian origin is necessary to establish the frequency of the c.1381 C>T variant in that population.

The *CDHR1* gene comprises 17 exons and encodes a protein of 859 amino acids. The novel c.1381 C>T nonsense variant is located in exon 13 of *CDHR1* and alters glutamine at 461 to a stop codon (CAG>TAG). This change is predicted to cause premature truncation of the protein, resulting in the loss of 397 C-terminal amino acids of the *CDHR1* protein. This nonsense mutation may also lead to nonsense-mediated decay of the transcript, resulting in loss of the protein.

CLINICAL EVALUATION

Review of the clinical and family history revealed autosomal recessive inheritance of RD in 3 offspring of consanguineous parents of Palestinian descent (Figure 1A). We studied 8 members of this pedigree spanning 3 generations, including the 3 sisters (IV-1, IV-3, and IV-4) affected with severe RD. The children of IV-3 and IV-4 were not examined but had no visual problems or symptoms by their parents' report. Three unexamined, unaffected siblings did not report visual problems.

OPHTHALMIC EVALUATION

Clinical findings are summarized in **Table 1**. The heterozygous mother (III-1) had visual acuity of 20/32 in the right eye resulting from a nuclear sclerotic cataract and 20/20 in the left eye; in V-1, visual acuity was 20/16 in each eye; visual fields and color vision were normal in each eye of both obligate heterozygous study participants. Family members with RD developed glare and photosensitivity during childhood; nyctalopia in adolescence; decreased contrast sensitivity, peripheral vision, and color vision loss in the third decade of life; and visual acuity loss in the fourth decade. The youngest affected member, IV-4, retained visual acuity of 20/40 in the right eye at age 32 years, although visual acuity in the left eye was reduced to 20/100. Color vision was abnormal in all affected members and showed diffuse color defects. **Figure 2A, D, G, and J** show the fundus appearance for the heterozygous mother, III-1, and 3 affected family members (IV-1, IV-3, and IV-4). Affected members showed a bull's eye pattern of retinal pigment epithelial (RPE) atrophy in the macula and circular patches of RPE atrophy anterior to the arcades, with retinal vascular attenuation and bone spicule pigmentation. In addition, IV-1 had glaucoma with an enlarged cup-disc ratio in each eye and mildly elevated intraocular pressure (21-24 mm Hg) beginning at age 40 years. Visual fields (Figure 2B, E, H, and K) were normal in III-1 but showed peripheral islands of vision temporally and inferiorly with central vision loss in IV-1 and severe constriction with small central islands in IV-3 and IV-4. The SD-OCT images (Figure 2C, F, I, and L) were obtained with horizontal scans through the anatomic fovea in each eye, with the exception of IV-1; a vertical scan was obtained as close as possible to the anatomic fovea. In all affected family members, SD-OCT (Figure 2F, I, and L) showed thinning and loss of the outer nuclear, IS, and

Table 1. Clinical and Molecular Characteristics of Affected and Unaffected Family Members Studied

Patient No./ Sex/Age at Visit, y	Nucleotide Changes at c.1381, No.	Protein Change of Q461Stop	Measurement in Right Eye, Left Eye				Desaturated Color Vision TES/CCI ^b
			Visual Acuity ^a	Refraction	Axial Length	Color Vision TCDS/CCI	
III-1/F/64	C/T	Heterozygous	20/32, 20/20	-3.00 + 1.00 × 005, plano + 0.40 × 180	23.57, 23.53	129.2/1.10, 117/1.00	32/1.23, 32/1.23
III-2/M/73	C/T	Heterozygous	20/20, 20/20	Plano, plano	NP	NP	NP
IV-1/F/45	T/T	Homozygous	20/1008, 20/800	-11.00 DS, -11.00 DS	23.29, 23.31	449.5/3.84, 382.4/3.27	NP
IV-2/F/37	C/T	Heterozygous	20/25, 20/25	NP, NP	NP	NP	NP
IV-3/F/36	T/T	Homozygous	20/160, 20/100	-2.00 + 1.00 × 120, -2.00 + 1.25 × 085	23.70, 23.70	Unable	Unable
IV-4/F/32	T/T	Homozygous	20/40, 20/100	-11.00 + 3.00 × 100, -10.50 + 3.00 × 085	24.73, 24.87	335.9/2.87, 347.6/2.97	NP
IV-5/F/25	C/T	Heterozygous	20/20, 20/20	Plano, plano	NP	NP	NP
V-1/M/21	NP	NP	20/16, 20/16	-0.25 DS, -0.25 DS	23.48, 23.69	117/1.00, 125.4/1.10	48/1.34, 0/1.00

Abbreviations: CCI, color confusion index (calculated as the total color difference score [TCDS] of the subject divided by the normal TCDS); NP, not performed; TES, total error score.

^aVisual acuity represents the best spectacle-corrected acuity.

^bA normal TES is lower than the 95% confidence level, which is 109 for age 64 years and 51 for age 21 years.

OS layers. However, the outer retinal layers were relatively preserved in the area surrounding the anatomic fovea in IV-3 and IV-4. In addition, SD-OCT images showed hyperreflective lesions within the attenuated outer nuclear layer in regions where the IS ellipsoid portion²⁰ or IS-OS junction was not observed in IV-4 (Figure 2L and **Figure 3F**, black arrows) and external to the external limiting membrane and IS ellipsoid or IS-OS junction in IV-3 and IV-4 (Figures 2F and L and 3F, red arrows). The clinically normal heterozygous mother, III-1, showed subtle disruptions in reflectivity of the OS-RPE junction (Figures 2C and 3D, red arrows) in a region that corresponded to mild RPE depigmentation on the color fundus photograph (Figures 2A and 3A, red arrows). The other heterozygous family member who underwent SD-OCT imaging was V-1; results of the scans were normal, without hyperreflective abnormalities (data not shown). Electroretinographic responses were within 2 SDs of the normal mean in the heterozygous carrier, III-1. In the homozygous individuals, both rod-mediated and cone-mediated responses were severely reduced below levels that can be reliably measured (**Figure 4** and **Table 2**).

Visual fixation was not stable enough in patients IV-1 and IV-3 to acquire images using AOSLO. However, IV-4 retained visual acuity of 20/40 in the right eye. The AOSLO images revealed coarse cone mosaics near the fovea, with increased cone spacing and reduced cone density (Figure 3E). Where cone mosaics were observed, permitting quantitative analysis, cone spacing was increased by 5 to 6 SDs above the normal mean (Figure 3E). Although the color fundus photographs appeared normal and cone spacing was normal throughout the region imaged using AOSLO where cone mosaics were clearly seen (Figure 3C), AOSLO images in III-1 showed a region in which normal cone mosaics were not observed within the central 4 degrees (Figure 3C, white asterisk). The findings corresponded to an area where the OS-RPE junction was disrupted on SD-OCT (Figures 2C and 3D, red arrow). These

changes may suggest focal, subclinical cone abnormalities in heterozygous carriers of mutations in the *CDHRI* gene who are older than 60 years.

COMMENT

Exome analysis of a single affected member of a recessive RD pedigree led to the identification of a novel homozygous nonsense change in the *CDHRI* gene segregating with the disease. Consistent with the phenotype of patients with *CDHRI* mutations, the affected members of the Palestinian pedigree developed retinal degeneration affecting rods and cones. Previously, 3 distinct protein-truncating mutations in the *CDHRI* gene have been implicated in causing RD in 2 Middle Eastern families and 1 consanguineous family from the Faroe Islands.^{11,12} Identification of an additional novel protein truncating change in the Palestinian pedigree with RD supports the hypothesis that loss of functional *CDHRI* leads to retinal dystrophy involving rod and cone degeneration.¹⁰⁻¹²

Individuals with the homozygous Gln461 stop change developed symptoms of glare and photophobia beginning in childhood, followed by loss of night vision and then peripheral vision, followed by severe central vision loss by the middle of the fourth decade of life. The oldest affected sibling, IV-1, retained significant peripheral islands of vision despite severe central vision loss; the 2 younger siblings retained only small central islands of vision. Other reports^{11,12} on patients with *CDHRI* mutations described considerable variation in visual field loss, color vision loss, and circular patches of RPE atrophy in the macula and periphery, as observed in the affected members of the Palestinian pedigree in the present report. As in previous reports, visual acuity loss progressed rapidly between the ages of 30 and 40 years in affected individuals, with acuity reduced to 20/100 or worse in all patients older than 32.

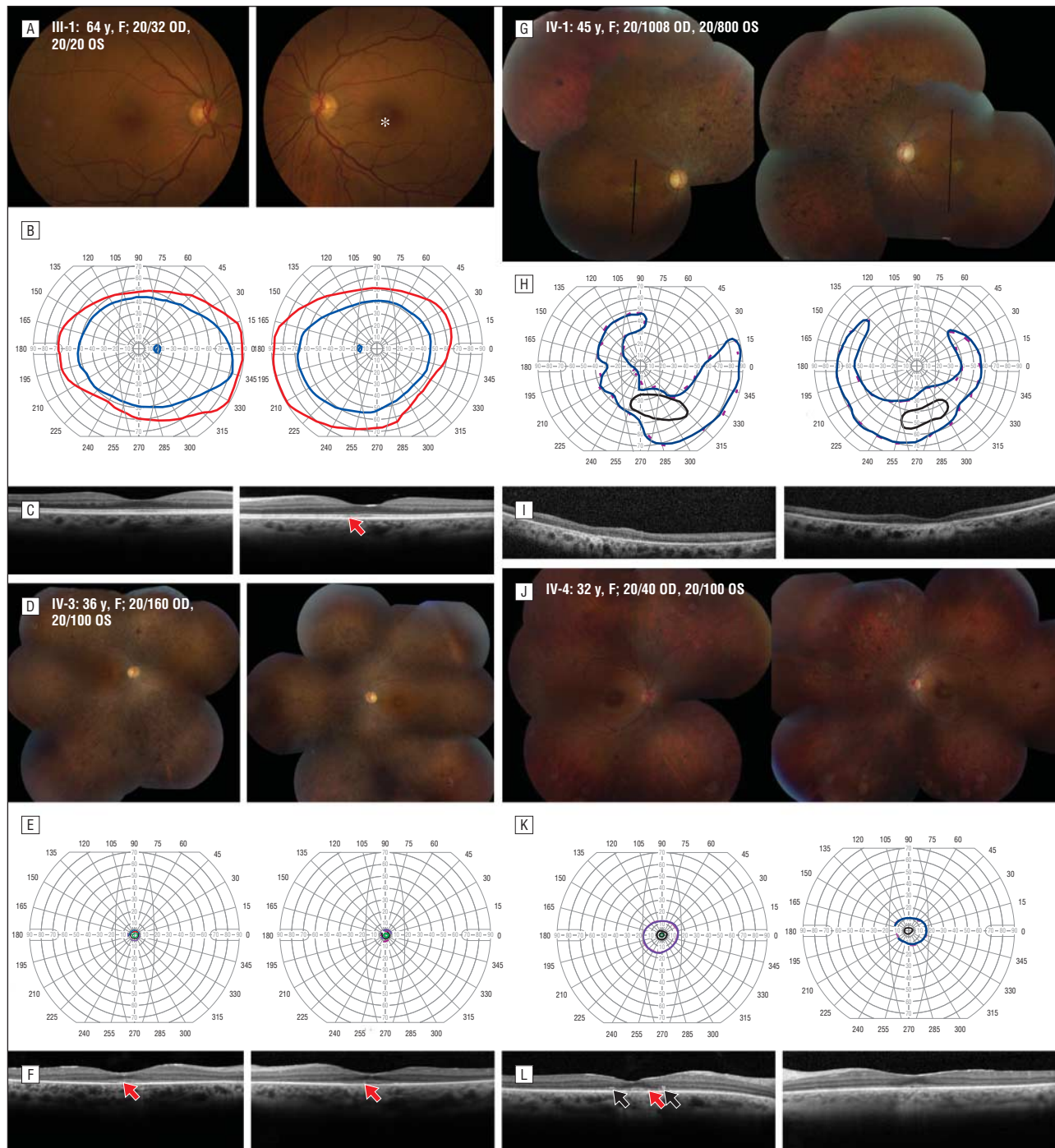


Figure 2. Clinical features in the affected family members. A, D, G, and J, Color fundus photographs. B, E, H, and K, Goldmann perimetry. C, F, I, and L, Spectral-domain optical coherence tomographic images through fixation, except in family member IV-1, where black lines indicate vertical scan location. Homozygotes show outer retinal loss with hyperreflective lesions in the outer nuclear layer (black arrows). The asterisk indicates a region of mild retinal pigment epithelial (RPE) depigmentation; red arrows, disrupted reflectivity of the outer segment–RPE junction and hyperreflective lesions external to the external limiting membrane and inner-segment ellipsoid band. OD indicates right eye; OS, left eye.

In 1 eye of IV-4, visual acuity remained 20/40 at age 32 years, providing an opportunity to study cones retained near the fovea using high-resolution imaging techniques. In the small central region where unambiguous cones were visualized, the cones showed increased spacing and reduced density. Cone mosaics were seen in regions where the IS ellipsoid portion or IS-OS junction was visualized, but at the site of the IS-OS disruption, cone mosaics were not observed. Although the pheno-

type of patients with RD resulting from *CDHR1* mutations affects both rods and cones, the retention of visual acuity and a small region of persistent cones near the fovea suggests that foveal cones are preserved until late in the degeneration process in some patients with *CDHR1* mutations, similar to the pattern observed in patients with RD caused by mitochondrial mutations, such as adenosine triphosphatase synthase 6, or mutations in rhodopsin or RDS.^{15,21,22} Therapeutic interventions aimed at pre-

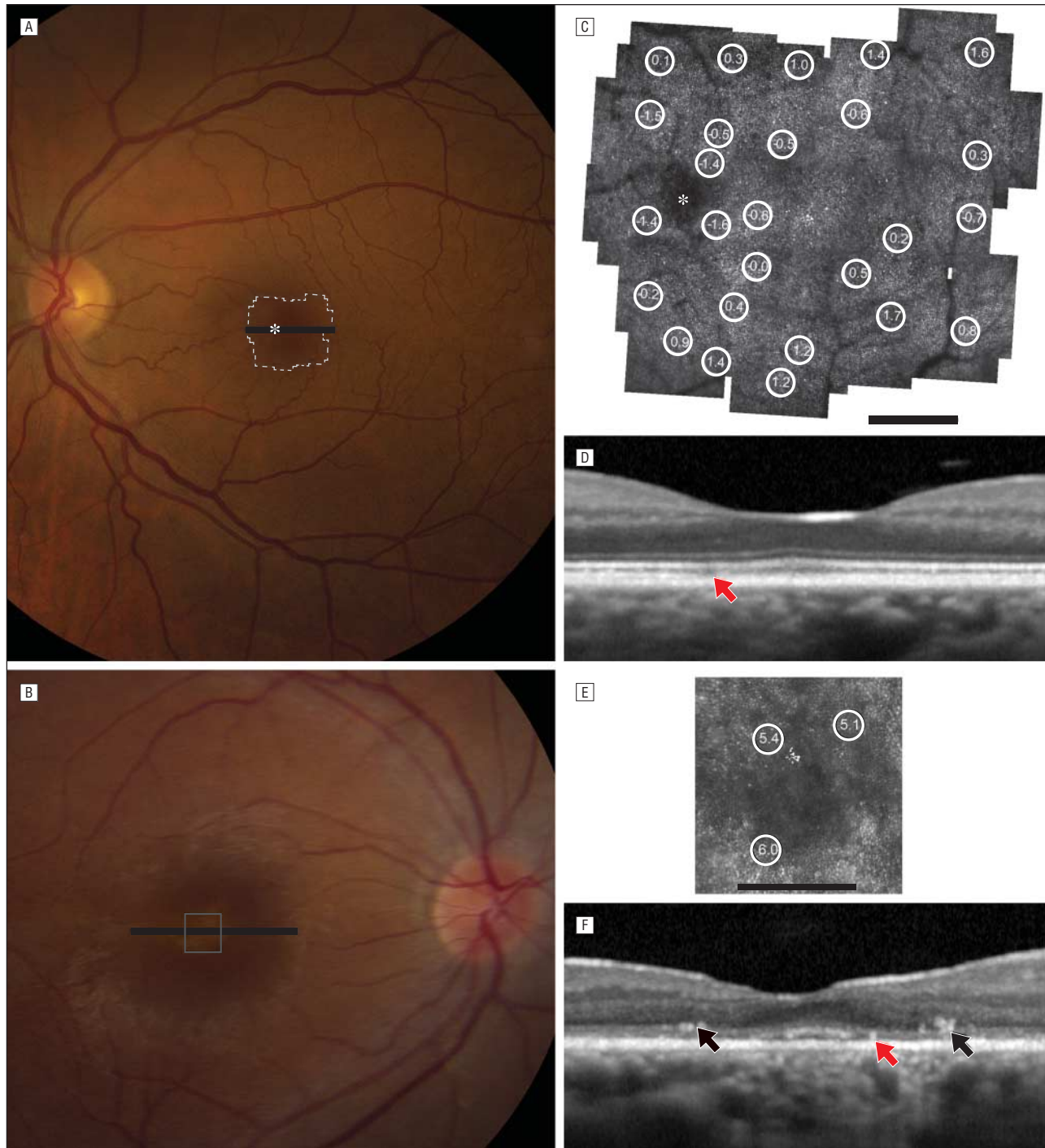


Figure 3. High-resolution foveal images. A, Color fundus photograph for family member III-1. B, Color fundus photograph for IV-4. C, Adaptive optics scanning laser ophthalmoscopy (AOSLO) image for III-1. D, Spectral-domain optical coherence tomography (OCT) for III-1. E, AOSLO image for IV-4. F, Spectral-domain OCT for IV-4. In family member III-1, cones are not seen in some regions (white asterisk, red arrow). In IV-4, the thin outer nuclear layer shows hyperreflective lesions and cone spacing is increased. The asterisks indicate a region of mild retinal pigment epithelial (RPE) depigmentation; circled numbers, standard deviations from the normal mean cone spacing; red arrows, subtle disruptions in the reflectivity of the outer segment-RPE junction; and black arrows, hyperreflective lesions in the outer nuclear layer. A and B, Bars indicate the spectral-domain OCT scan location. C and E, Scale bars represent 1°.

serving cone structure, either through gene replacement or neurotrophic factors, might be most beneficial if administered to patients who retain central cones and have visual acuity no worse than 20/40.²¹ High-resolution imaging techniques such as AOSLO may provide a sensitive means of monitoring disease progression and response to experimental therapies in patients

with *CDH1* mutations who retain central visual acuity better than 20/100.

The *CDH1* gene has been shown to play an essential role in photoreceptor OS disc morphogenesis. In mice with null *CDH1* mutations, OS discs are fragmented and disorganized, although protein transport from the IS to the OS and phototransduction are not affected.¹⁰ The pres-

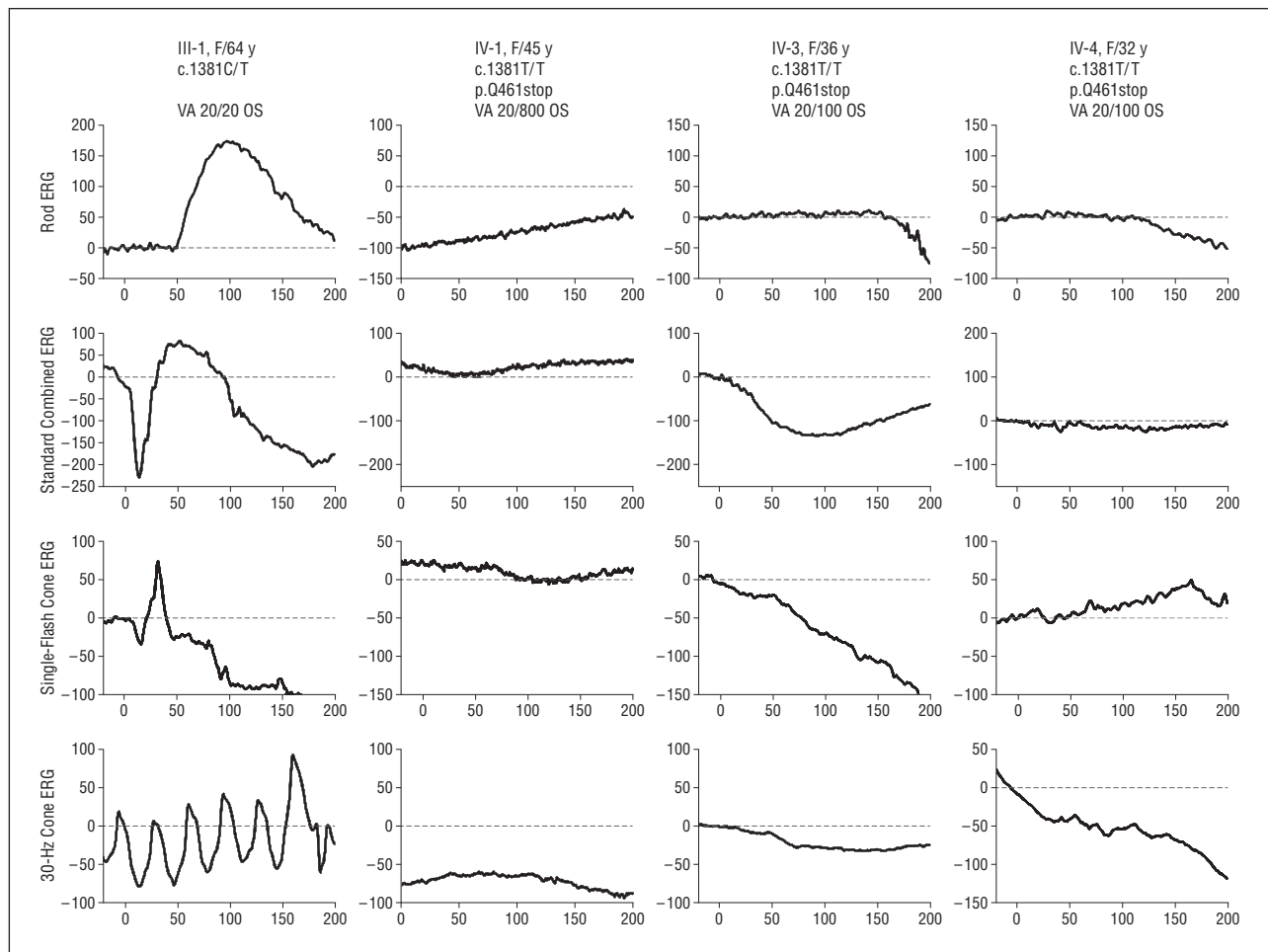


Figure 4. International Society for Clinical Electrophysiology of Vision standard full-field electroretinography (ERG) in the family members studied. Rod- and cone-mediated ERG responses were severely reduced in the affected members (IV-1, IV-3, and IV-4) but were within 2 SDs of the normal mean in the heterozygous carrier (III-1). OS indicates left eye; VA, visual acuity.

Table 2. Full-Field Electroretinographic Findings in Left Eyes of Family Members Studied

Subject No./ Age at Visit, y	Amplitude, μV /Implicit Time, ms^a					
	Dim Scotopic (Rod) B-Wave	Bright Scotopic (Combined) A-Wave	Bright Scotopic (Combined) B-Wave	Single-Flash Photopic (Cone) A-Wave	Single-Flash Photopic (Cone) B-Wave	30-Hz Flicker Photopic (Cone)
III-1/64	177.1/97	154.0/17	310.3/52	34.3/16	108.0/32	85.1/28
IV-1/45	ND	ND	ND	ND	ND	ND
IV-3/36	ND	ND	ND	ND	ND	ND
IV-4/32	ND	ND	ND	ND	ND	ND

Abbreviation: ND, not detectable at criterion levels of 3 μV for all responses except for 30-Hz photopic flicker, where the criterion was 0.1 μV .

^aNormal mean (SD) electroretinographic dim scotopic b-wave amplitude is 281 (70) μV ; mixed scotopic a-wave amplitude, 210 (54) μV ; mixed scotopic b-wave amplitude, 422 (100) μV ; single-flash cone a-wave amplitude, 38 (11) μV ; single-flash cone b-wave amplitude, 147 (46) μV ; and 30-Hz flicker cone amplitude, 120 (36) μV . Normal mean (SD) dim scotopic b-wave timing is 95 (7) milliseconds; mixed scotopic a-wave timing, 19 (3) milliseconds; mixed scotopic b-wave timing, 53 (3) milliseconds; single-flash cone a-wave timing, 15 (1) milliseconds; single-flash cone b-wave timing, 32 (2) milliseconds; and cone flicker timing, 28 (2) milliseconds.

ent study contributes information about outer retinal structure in living human eyes with *CDHR1* mutations predicted to result in a lack of functional protein. In the affected family members studied, SD-OCT images revealed highly reflective structures at the edges of the attenuated outer nuclear layer. Beneath the anatomic fovea, where outer retinal structure was relatively preserved in the 2 youngest affected siblings homozygous for the

CDHR1 Gln461 stop change, hyperreflective lesions were observed outside the external limiting membrane (red arrows, Figures 2 and 3). These hyperreflective lesions may represent the SD-OCT depiction of fragmented, disorganized OS in humans with *CDHR1* mutations.

In the clinically normal heterozygous mother of the affected siblings, III-1, SD-OCT showed some hyporeflexive irregular regions external to the IS ellipsoids or

IS-OS junction (red arrows, Figures 2C and 3D) in regions where unambiguous cone mosaics were not visualized using AOSLO (white asterisk, Figures 2A, 3A, and 3C). These features may represent common age-related changes, but they were not associated with drusen on the color fundus photographs or SD-OCT images and may represent subtle manifestations of the heterozygous *CDHR1* carrier state present at age 64 years. Homozygous mutations in the gene encoding PROM1, which interacts with *CDHR1* to enable normal photoreceptor OS structure, have been reported^{23,24} in patients with autosomal recessive RD, characterized by narrowed arteries, optic disc pallor, pigment deposits, and macular degeneration. A heterozygous carrier of this mutation developed unilateral macular degeneration with vision loss in the fifth decade of life,²⁴ perhaps similar to the subtle changes observed in III-1 in the present study.

In summary, we characterized the retinal phenotype in patients with autosomal recessive RD caused by a novel nonsense change in the *CDHR1* mutation. Retinal degeneration in individuals homozygous for this change is severe, resulting in extensive central vision loss by the middle of the fourth decade of life. Cones were observed near the fovea in 1 eye of the youngest affected individual at age 32 years in whom visual acuity was 20/40. Imaging with SD-OCT in homozygous family members with RD demonstrated outer retinal hyperreflective lesions that may represent the human correlate of the disrupted, fragmented photoreceptor OS observed in mice with *CDHR1* mutations. With previously reported findings, this study supports the hypothesis that *CDHR1* is important for normal photoreceptor OS structure and survival. Furthermore, these studies establish the value of exome sequencing in identifying private causative variants in genes involved in causing RD.

Submitted for Publication: March 18, 2012; final revision received April 26, 2012; accepted April 30, 2012.

Correspondence: Radha Ayyagari, PhD, Shiley Eye Center, University of California San Diego, Jacobs Retina Center, 9415 Campus Point Dr, Room 206, San Diego, CA 92093 (rayyagari@ucsd.edu).

Author Contributions: Dr Ayyagari had full access to all the data in the study and takes responsibility for the integrity of the data and the accuracy of the data analysis.

Financial Disclosure: Dr Roorda holds a patent on adaptive optics scanning laser ophthalmoscopy (US patent 7118216).

Funding/Support: This work was supported by the Core Grant for Vision Research EY002162 from the NIH and National Eye Institute, That Man May See, Inc, The Bernard A. Newcomb Macular Degeneration Research Fund, and The American Health Assistance Fund (Dr Duncan); Foundation Fighting Blindness and Research to Prevent Blindness (Drs Duncan and Ayyagari); The Beutler Foundation (Dr Lee); and grants NIH-EY013198 (Dr Ayyagari), NIH-EY021237 (Dr Ayyagari), and NIH-EY020678 (Dr Gaasterland) from the NIH.

Additional Contributions: Steve Head, MS, Sandra Soares, and Lee Edsall, MS, provided valuable assistance in exome sequencing and analysis of the proband and John Suk,

BS, provided excellent technical assistance (all were paid staff members). We thank all participants in this study.

REFERENCES

- RetNet: summary of genes and loci causing retinal diseases. <https://sph.uth.tmc.edu/Retnet/sum-dis.htm>. Accessed January 8, 2012.
- Briggs CE, Rucinski D, Rosenfeld PJ, Hirose T, Berson EL, Dryja TP. Mutations in *ABCR (ABCA4)* in patients with Stargardt macular degeneration or cone-rod degeneration. *Invest Ophthalmol Vis Sci*. 2001;42(10):2229-2236.
- Wells J, Wroblewski J, Keen J, et al. Mutations in the human retinal degeneration slow (*RDS*) gene can cause either retinitis pigmentosa or macular dystrophy. *Nat Genet*. 1993;3(3):213-218.
- McGee TL, Seyedahmadi BJ, Sweeney MO, Dryja TP, Berson EL. Novel mutations in the long isoform of the *USH2A* gene in patients with Usher syndrome type II or non-syndromic retinitis pigmentosa. *J Med Genet*. 2010;47(7):499-506.
- Boon CJ, Klevering BJ, Leroy BP, Hoyng CB, Keunen JE, den Hollander AI. The spectrum of ocular phenotypes caused by mutations in the *BEST1* gene. *Prog Retin Eye Res*. 2009;28(3):187-205.
- Bamshad MJ, Ng SB, Bigham AW, et al. Exome sequencing as a tool for Mendelian disease gene discovery. *Nat Rev Genet*. 2011;12(11):745-755.
- Ng SB, Turner EH, Robertson PD, et al. Targeted capture and massively parallel sequencing of 12 human exomes. *Nature*. 2009;461(7261):272-276.
- Tucker BA, Scheetz TE, Mullins RF, et al. Exome sequencing and analysis of induced pluripotent stem cells identify the cilia-related gene male germ cell-associated kinase (*MAK*) as a cause of retinitis pigmentosa. *Proc Natl Acad Sci U S A*. 2011;108(34):E569-E576.
- Rattner A, Chen J, Nathans J. Proteolytic shedding of the extracellular domain of photoreceptor cadherin: implications for outer segment assembly. *J Biol Chem*. 2004;279(40):42202-42210.
- Rattner A, Smallwood PM, Williams J, et al. A photoreceptor-specific cadherin is essential for the structural integrity of the outer segment and for photoreceptor survival. *Neuron*. 2001;32(5):775-786.
- Henderson RH, Li Z, Abd El Aziz MM, et al. Biallelic mutation of protocadherin-21 (*PCDH21*) causes retinal degeneration in humans. *Mol Vis*. 2010;16:46-52.
- Ostergaard E, Batbayli M, Duno M, Vilhelmsen K, Rosenberg T. Mutations in *PCDH21* cause autosomal recessive cone-rod dystrophy. *J Med Genet*. 2010;47(10):665-669.
- Bowman KJ. A method for quantitative scoring of the Farnsworth panel D-15. *Acta Ophthalmol (Copenh)*. 1982;60(6):907-916.
- Lanthon P. Evaluation of the desaturated panel D-15: I: method of quantification and normal scores. *J Fr Ophtalmol*. 1986;9(12):843-847.
- Duncan JL, Talcott KE, Ratnam K, et al. Cone structure in retinal degeneration associated with mutations in the peripherin/RDS gene. *Invest Ophthalmol Vis Sci*. 2011;52(3):1557-1566.
- Marmor MF, Holder GE, Seeliger MW, Yamamoto S; International Society for Clinical Electrophysiology of Vision. Standard for clinical electroretinography (2004 update). *Doc Ophthalmol*. 2004;108(2):107-114.
- Duncan JL, Zhang Y, Gandhi J, et al. High-resolution imaging with adaptive optics in patients with inherited retinal degeneration. *Invest Ophthalmol Vis Sci*. 2007;48(7):3283-3291.
- Roorda A, Zhang Y, Duncan JL. High-resolution in vivo imaging of the RPE mosaic in eyes with retinal disease. *Invest Ophthalmol Vis Sci*. 2007;48(5):2297-2303.
- dbSNP: short genetic variations. <http://www.ncbi.nlm.nih.gov/projects/SNP>. Accessed January 4, 2012.
- Spaide RF, Curcio CA. Anatomical correlates to the bands seen in the outer retina by optical coherence tomography: literature review and model. *Retina*. 2011;31(8):1609-1619.
- Talcott KE, Ratnam K, Sundquist SM, et al. Longitudinal study of cone photoreceptors during retinal degeneration and in response to ciliary neurotrophic factor treatment. *Invest Ophthalmol Vis Sci*. 2011;52(5):2219-2226.
- Yoon MK, Roorda A, Zhang Y, et al. Adaptive optics scanning laser ophthalmoscopy images in a family with the mitochondrial DNA T8993C mutation. *Invest Ophthalmol Vis Sci*. 2009;50(4):1838-1847.
- Yang Z, Chen Y, Lillo C, et al. Mutant prominin 1 found in patients with macular degeneration disrupts photoreceptor disk morphogenesis in mice. *J Clin Invest*. 2008;118(8):2908-2916.
- Maw MA, Corbeil D, Koch J, et al. A frameshift mutation in prominin (mouse)-like 1 causes human retinal degeneration. *Hum Mol Genet*. 2000;9(1):27-34.